

Gold(III)-Dithiocarbamate Complexes Induce Cancer Cell Death Triggered by Thioredoxin Redox System Inhibition and Activation of ERK Pathway

Daniela Saggioro,^{1,7} Maria Pia Rigobello,^{2,7} Lucia Paloschi,³ Alessandra Folda,² Stephen A. Moggach,⁴ Simon Parsons,⁴ Luca Ronconi,^{4,5} Dolores Fregona,^{5,8,*} and Alberto Bindoli^{6,8,*}

¹Molecular Immunology and Diagnostic Oncology, Istituto Oncologico Veneto I.R.C.C.S., Via Gattamelata 64, Padova 35128, Italy

²Department of Biological Chemistry, University of Padova, V.le G. Colombo 3, Padova 35121, Italy

³Department of Oncology and Surgical Sciences, University of Padova, Via Gattamelata 64, Padova 35128, Italy

⁴School of Chemistry, University of Edinburgh, West Mains Road, Edinburgh EH9 3JJ, United Kingdom

⁵Department of Chemical Sciences, University of Padova, Via Marzolo 1, Padova 35131, Italy

⁶Institute of Neurosciences, C.N.R., V.le G. Colombo 3, Padova 35121, Italy

⁷These authors contributed equally to this work.

⁸These authors are co-senior authors.

*Correspondence: dolores.fregona@unipd.it (D.F.), alberto.bindoli@bio.unipd.it (A.B.)

DOI 10.1016/j.chembiol.2007.08.016

SUMMARY

Although gold compounds are now recognized as promising anticancer agents, so far only gold(I) derivatives have been investigated for this purpose, whereas the use of gold(III) complexes has been hampered by their poor stability under physiological conditions. We have therefore carried out studies on selected gold(III) anticancer agents, showing enhanced stability due to the presence of chelating dithiocarbamate ligands. We found that they induce cancer cell death through both apoptotic and nonapoptotic mechanisms. They also inhibit thioredoxin reductase activity, generate free radicals, modify some mitochondrial functions, and increase ERK1/2 phosphorylation. Based on our results, we propose and discuss a working model suggesting that deregulation of the thioredoxin reductase/thioredoxin redox system is a major mechanism involved in the anticancer activity of the investigated gold(III)-dithiocarbamate complexes.

INTRODUCTION

The treatment of a variety of cancers by platinum derivatives has encouraged the continuous investigation of alternative metal-based drugs. Owing to their anti-inflammatory and immunosuppressive properties, some gold(I) compounds used for the treatment of rheumatoid arthritis [1–3] were considered for their possible anticancer activity. Indeed, some of the clinically established antiarthritic gold(I) compounds, such as gold(I) thiomalate (myocrisin), gold(I) thioglucose (solganol), and 2,3,4,6-tetra-*o*-acetyl-1-thio- β -D-glucopyranosato-(S)-triethylphosphine gold(I)

(auranofin), were found to exert significant antitumor activity both in vitro and in vivo [4–10].

So far, while the potential anticancer action of gold(I) derivatives has been widely investigated, the development of gold(III) complexes as alternative antitumor agents has been hampered by their poor stability under physiological conditions. Although the stability of gold(III) metal center may be enhanced by the coordination of multidentate ligands, the excess of stabilization may result in a loss of biological activity [11]. Nevertheless, recent studies showed that some selected gold(III) complexes are able to exert outstanding cytotoxic activity toward various tumor cell lines with IC₅₀ values falling in the range 1–10 μ M [11–16].

In order to understand the mechanism of action of anticancer agents, it is of paramount importance to identify the molecular components involved in the cascade of events that finally trigger cell death.

In light of the close chemical similarity between platinum and gold compounds, it was believed that both might target DNA. However, in addition to a direct interaction with DNA in vitro [17], both gold(I) and gold(III) complexes have been reported to interact with other cellular components. Recently, we have reported on the antiproliferative and apoptotic activities of two gold(III)-methylsarcosinedithiocarbamate derivatives toward a panel of human myeloid leukemia cell lines. These novel gold(III) complexes appear to induce a strong downregulation of the antiapoptotic Bcl-2 molecule and an upregulation of the proapoptotic Bax protein, but only weak perturbations of the cell cycle [18]. This behavior diverges from that of the classical platinum(II) complexes which, instead, induce cell cycle alterations resulting in an increase in G2M cell fraction [19]. Furthermore, we have identified the proteasome as a possible in vitro and in vivo target of gold(III)-dithiocarbamate derivatives such as complexes 1 and 4 (Figure 1A). The inhibition of the proteasomal chymotrypsin-like activity results in the accumulation of ubiquitinated proteins and the proteasome target protein p27 in the highly metastatic MDA-MB-231 human Caucasian breast adenocarcinoma

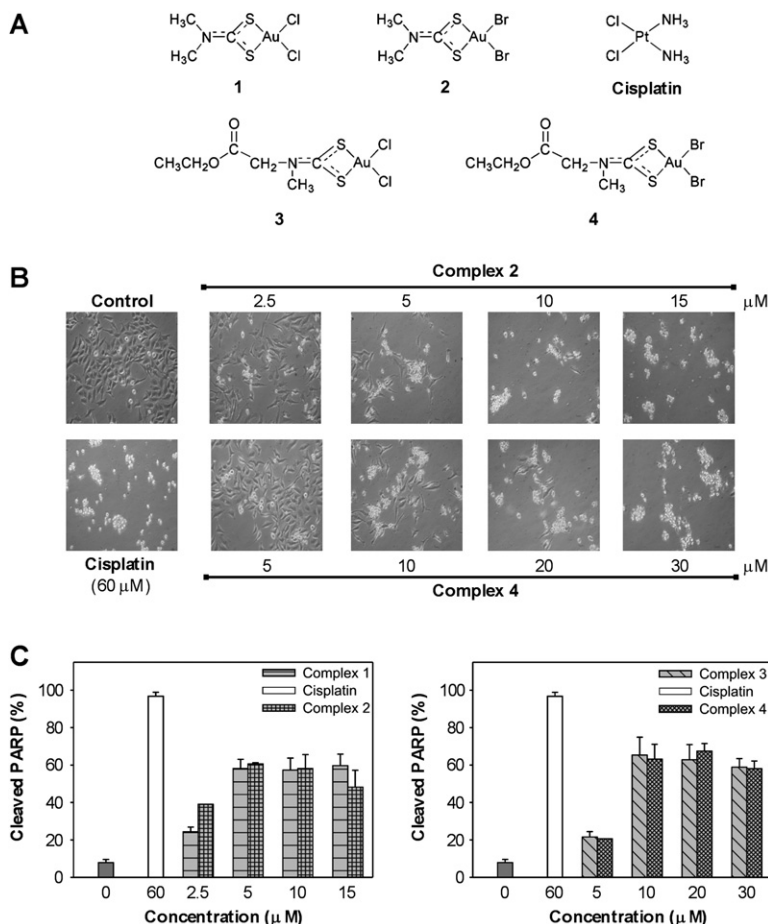


Figure 1. Chemical Drawings of the Investigated Gold(III)-Dithiocarbamate Complexes and Determination of the Apoptotic Effects on HeLa Cells

(A) Investigated complexes: $[\text{Au}(\text{DMDT})\text{Cl}_2]$ (1), $[\text{Au}(\text{DMDT})\text{Br}_2]$ (2), $[\text{Au}(\text{ESDT})\text{Cl}_2]$ (3), $[\text{Au}(\text{ESDT})\text{Br}_2]$ (4). Structure of the reference drug cisplatin ($\text{cis-}[\text{PtCl}_2(\text{NH}_3)_2]$) is also reported for clarity.

(B) Phase-contrast microscopy representative pictures of cell death after treatment with different concentrations of complexes 2 (2.5/5/10/15 μM) and 4 (5/10/20/30 μM), and cisplatin (60 μM) for 24 h. Original magnification = 100 \times . (C) Quantification of apoptosis through PARP cleavage determination. After 24 hr treatment the cells were collected, lysed, and aliquots of total proteins subjected to western blot analysis of PARP cleavage. Percentage of PARP cleavage was calculated as the ratio between densitometrical values of cleaved and un-cleaved bands $\times 100$. Values are given as means \pm SE of at least three independent experiments.

cell line. In addition, treatment of MDA-MB-231 tumor-bearing nude mice resulted in a significant inhibition of tumor growth, associated to the inhibition of proteasome activity and the massive induction of apoptosis *in vivo* [20].

On the other hand, recent data have identified mitochondria as suitable targets for gold complexes to exert their cytotoxicity, as recently reviewed by McKeage et al. [6]. In particular, mitochondrial thioredoxin reductase appears to be a very specific target for gold(I) complexes, such as auranofin, aurothiomalate, and other gold(I)-triethylphosphine derivatives [21], and gold(III) complexes containing diethylendiamino-substituted pyridino and bipyridino ligands [22, 23]. This finding is highly significant as mitochondria are now taken into account as potential targets for chemotherapeutic drugs due to their well-known key role in apoptosis.

As a natural continuation of our previous studies, we here report on the effect of some recently synthesized gold(III)-dithiocarbamate derivatives, namely $[\text{Au}(\text{DMDT})\text{X}_2]$ and $[\text{Au}(\text{ESDT})\text{X}_2]$ (DMDT = *N,N*-dimethyldithiocarbamate; ESDT = ethylsarcosinedithiocarbamate; X = Cl, Br) (Figure 1A) [15], on cell cytotoxicity and mitochondrial functions. Analyses were carried out at molecular, subcellular, and cellular levels. We found that they trigger cell death by activating both apoptotic and nonapoptotic pathways. They alter some mitochondrial functions such

as membrane potential and permeability conditions, stimulate ROS generation, and are particularly effective in inhibiting the activity of selenoenzyme thioredoxin reductase with similar or even higher efficiency compared to other gold(III) complexes [22, 24]. Intriguingly, we have evidence that treatment of HeLa cells with these gold(III)-dithiocarbamate complexes induces phosphorylation of ERK, and that ERK activation can be completely blocked by the antioxidant *N*-acetyl-L-cysteine (NAC), whereas treatment with Trolox is ineffective. Based on our findings, we propose and discuss a working model of the molecular mechanisms involved in the cell death induced by the investigated gold(III) anticancer agents.

RESULTS

X-Ray Crystallography

The complexes $[\text{Au}(\text{DMDT})\text{X}_2]$ [X = Cl (1), Br (2)] and $[\text{Au}(\text{ESDT})\text{X}_2]$ [X = Cl (3), Br (4)] (Figure 1A) have been designed to reproduce very closely the main features of cisplatin. Conclusions reached upon application of several spectroscopic techniques suggest that coordination of both DMDT and ESDT ligands takes place in a near square-planar geometry through the sulfur-donating atoms, with the NCSS moiety coordinating the metal center in a bidentate symmetrical mode. The remaining

coordination positions are occupied by two *cis*-gold(III)-halogen atoms that may undergo hydrolysis [15]. This structural hypothesis is also supported by density functional calculations previously carried out for some analogous gold(III)-dithiocarbamate complexes [25]. In addition, we recently determined the X-ray structure of complex 4, which is in agreement with the previously reported spectroscopic data (see the [Supplemental Data](#) available with this article online).

Apoptotic Activity

The apoptotic activity of complexes 1–4 was evaluated on human cervical carcinoma HeLa cells incubated for 24 h with increasing drug concentrations. Concentrations ranged from 2.5 to 15 μ M and from 5 to 30 μ M for DMDT (1 and 2) and ESDT (3 and 4) derivatives, respectively, with their IC_{50} values (concentration of drug resulting in 50% inhibition of cell growth) being slightly different toward the same human tumor cell lines [15, 16]. Cisplatin was also tested as a reference drug. Analysis of cultures after the treatment showed that both DMDT and ESDT gold(III) derivatives were able to induce cell death in a dose-dependent way (Figure 1B); no substantial differences were observed among chloro- and bromo-derivatives containing the same dithiocarbamate ligand.

To determine whether the observed cell death was due to the activation of an apoptotic pathway, we analyzed the poly-(ADP-ribose)-polymerase (PARP) cleavage. PARP is a nuclear enzyme, activated by DNA damage, involved in DNA repair, cell death, and inflammation [26]. Moreover, PARP is a specific substrate for caspases 3 and 7; therefore, PARP cleavage is generally accepted as a marker for apoptosis [27]. Indeed, apoptosis is a form of cell death characterized by the activation of caspases (cysteine-specific protease) that cleave multiple targets in the cell. Thus, after microscope observation, the cells were collected, lysed, and total proteins subjected to western blot analysis. As shown in Figure 1C, the percentage of PARP cleavage after 24 hr treatment, quantified by densitometric analysis, was nearly the same for all tested gold(III) complexes and, surprisingly, non-dose-dependent (except for lower dose treatments). These findings contrast with those obtained from the morphological examination of the cultures, in which the cell death appeared to be dose-dependent (Figure 1B). Thus, it is likely that our compounds may trigger cell death by activating not only apoptotic pathways but also other death mechanisms (i.e., necrosis). On the contrary, cells treated with cisplatin induced a complete PARP cleavage, confirming that the reference drug leads to cell death only through an apoptotic pathway.

Effects on Mitochondrial Functions

Although mitochondria have long been considered to be solely a powerhouse for production of cellular energy, recently they have been clearly recognized to play a critical role in the apoptotic process [28]. Therefore, the physiological consequences on the mitochondrial respiratory parameters, membrane potential, and permeability transi-

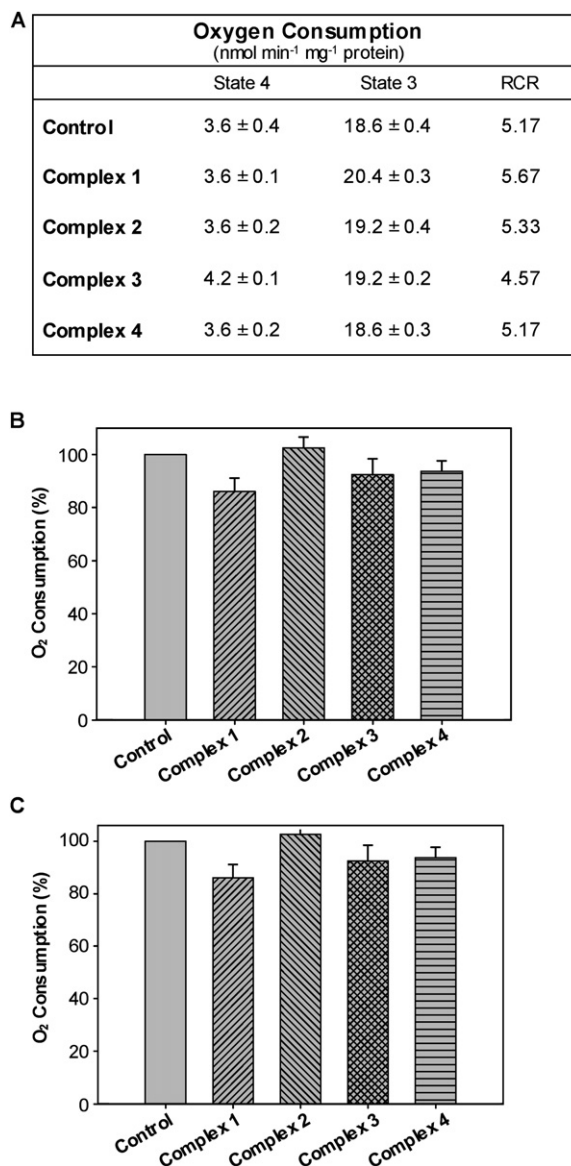


Figure 2. Oxygen Uptake by Rat Liver Mitochondria and Sub-mitochondrial Particles

Rat liver mitochondria (A) or submitochondrial particles (B and C) were incubated at 25°C with complexes 1–4 to a final concentration of 5 μ M for mitochondria and 10 μ M for submitochondrial particles in the suitable medium (see [Experimental Procedures](#)). For submitochondrial particles either succinate (B) or NADH (C) were used as substrates. Oxygen consumption was measured as reported in the [Experimental Procedures](#) section. Respiration control ratio (RCR) was calculated as respiration rate in state 3/respiration rate in state 4. Values are given as means \pm SE of at least three independent experiments.

tion conditions after treatment with complexes 1–4 were studied. As summarized in Figure 2A, the respiratory control ratio (RCR) measured in whole mitochondria is scarcely affected, and uncoupled respiration shows a limited inhibition (data not shown), thus indicating that the electron flow along the respiratory chain is not significantly affected. In agreement with these observations, in

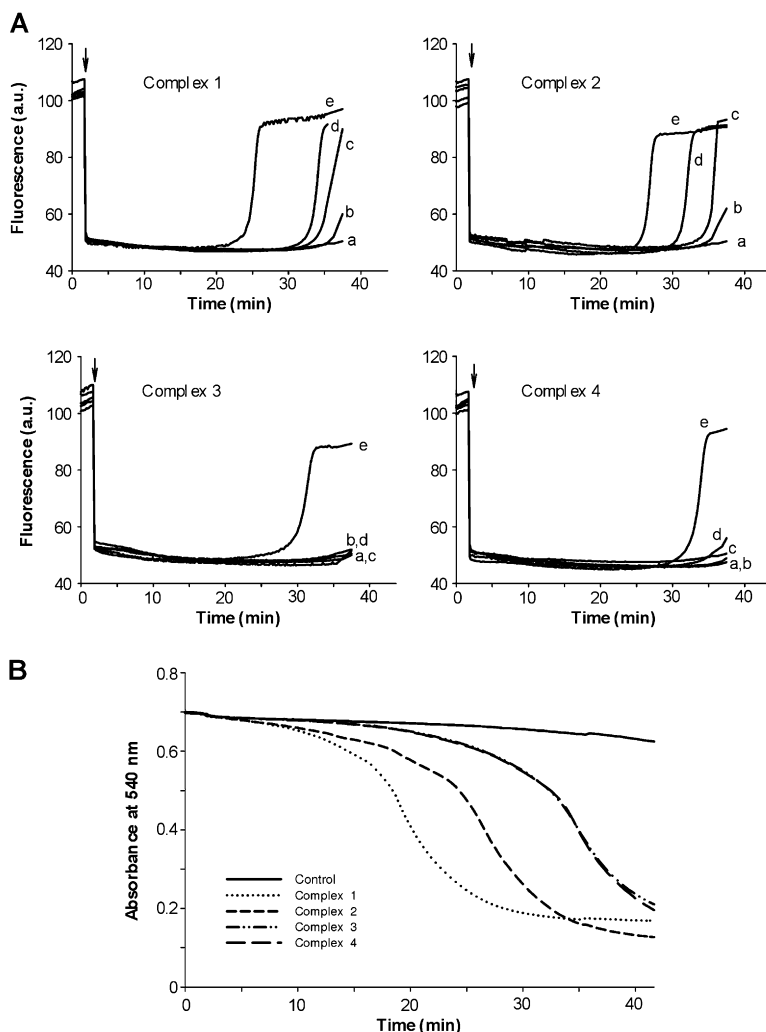


Figure 3. Effect on Mitochondrial Membrane Potential and Swelling

(A) Mitochondrial membrane potential was estimated as reported in the [Experimental Procedures](#). Mitochondria were energized by the addition of 5 mM succinate (arrow). Concentration of gold(III) complexes was: 0 (a), 1 μ M (b), 2 μ M (c), 3 μ M (d), 5 μ M (e). Values are reported as relative fluorescence units.

(B) Induction of mitochondrial swelling was estimated as described in the [Experimental Procedures](#) with complexes 1–4 to a final concentration of 2 μ M.

submitochondrial particles the respiration is modified by approximately 10%–20% after treatment with the various gold(III) complexes [using either succinate ([Figure 2B](#)) or reduced nicotinamide adenine dinucleotide (NADH, [Figure 2C](#)) as substrates]. Similarly to the observed apoptotic effect toward HeLa cells (see above), negligible differences were detected among chloro- and bromo-derivatives containing the same dithiocarbamate ligand.

Interestingly, different results were obtained when the membrane potential was estimated ([Figure 3A](#)). In fact, whereas complexes 1 and 2 caused a marked drop of membrane potential after about 20 to 30 min have elapsed, complex 4 was able to depolarize membrane after about 32 min of incubation, and complex 3 showed an intermediate behavior. In addition, all the investigated gold(III)-dithiocarbamate derivatives exhibit a marked effect when permeability transition, measured in terms of mitochondrial swelling, was taken into account. As reported in [Figure 3B](#), a large swelling is apparent after incubation with complexes 1–4; nevertheless, it is worth noting that swelling is faster in the presence of the two DMDT derivatives (1 and 2), whereas a longer lag occurs in the case

of ESDT derivatives (3 and 4), which take a longer time to accomplish the swelling. As well as the swelling induced by auranofin [21], also in this case swelling is dependent on the presence of a low concentration of calcium ions as observed by the inhibitory effect elicited by calcium chelators (EGTA) or inhibitors of mitochondrial calcium uptake such as ruthenium red (data not shown).

Estimation of ROS Accumulation in Isolated Mitochondria and HeLa Cells

The effect of complexes 1–4 on the production of reactive oxygen species (ROS), in particular hydrogen peroxide, in isolated rat liver mitochondria is shown in [Figures 4A](#) and [4B](#). As apparent, the addition of any of the complexes 1–4 strongly stimulates the formation of hydrogen peroxide, detected by means of Amplex Red/HRP (10 acetyl-3,7-dihydroxyphenoxazine/horseradish peroxidase) assay. The formation of hydrogen peroxide is further increased when antimycin is added ([Figure 4A](#)). By inhibiting the mitochondrial complex III, antimycin favors the production of superoxide anion which, after dismutation, is converted to hydrogen peroxide. Analogously, when antimycin is

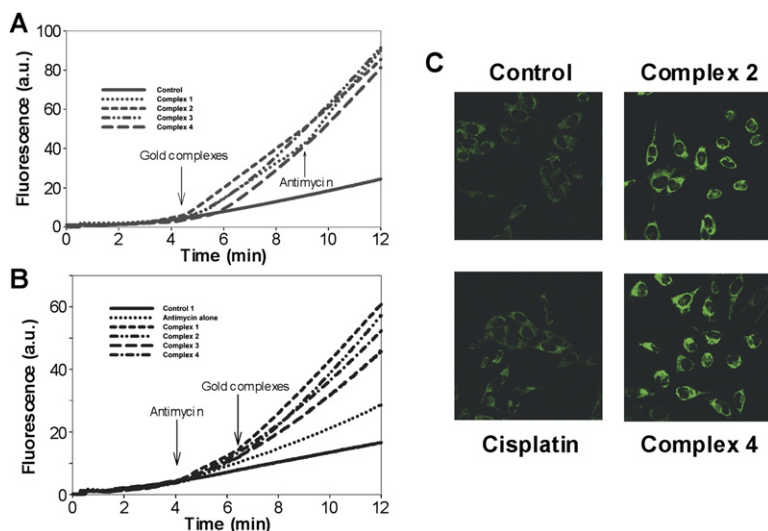


Figure 4. Evolution of Hydrogen Peroxide in Isolated Rat Liver Mitochondria and in Cultured HeLa Cells

Hydrogen peroxide formed by exposure of isolated rat liver mitochondria to complexes **1–4**. The fluorogenic probe Amplex Red and HRP were used at concentration of 10 μ M and 0.1 units/ml, respectively. The extent of hydrogen peroxide evolution was reported as relative fluorescence units. Antimycin (1 μ M) was added after (A) or before (B) the various gold(III) complexes (1 μ M). (C) ROS formation in HeLa cells was determined using the oxidation-sensitive probe DHR-123. Cells were loaded with DHR-123 (5 μ M) for 30 min, and then exposed to complexes **2** and **4** (10 μ M) for an additional 30 min. For comparison purposes, cisplatin (60 μ M) was tested under the same experimental conditions. ROS generation was examined using a Zeiss LSM-510 confocal laser microscope equipped with a CO₂- and temperature-controlled chamber.

added before incubating mitochondria with any of the investigated gold(III) complexes (Figure 4B), again they further stimulate the formation of hydrogen peroxide. The effectiveness of the four complexes is rather similar, although the two DMDT derivatives seem to be slightly more efficient than the ESDT counterparts.

As experiments carried out in isolated rat liver mitochondria showed that complexes **1–4** are able to induce formation of hydrogen peroxide, we checked whether these complexes trigger ROS generation also in HeLa cells. Intracellular ROS were detected using the oxidation-sensitive probe dihydrorhodamine-123 (DHR-123), which is reported to react preferentially with hydrogen peroxide and to localize at the mitochondrial level. Results, reported in Figure 4C, showed that the treatment with complexes **2** and **4** increases the oxidized state of the cells, detected as enhancement of fluorescence intensity of the probe; similar results were obtained with complexes **1** and **3** (data not shown). Conversely, control nontreated cells or cells treated with cisplatin showed only a weak fluorescent background, most likely due to small DHR-123 oxidation occurring during its manipulation. Thus, these results indicate that our gold(III) complexes are able to induce ROS in both isolated mitochondria and cells.

Effect of the Antioxidants Trolox and NAC on ROS Production and PARP Cleavage in HeLa Cells

To investigate whether ROS were responsible for the observed cell death, HeLa cells were treated in the presence of either NAC or the hydrophilic form of vitamin E (Trolox, 6-hydroxy-2,5,7,8-tetramethylchroman-2-carboxylic acid). Both are good ROS scavengers. NAC is a reducing thiol that helps to maintain the cellular thiol redox balance, whereas Trolox interacts preferentially with free radicals such as the peroxy radicals. Given that all four complexes exhibited similar apoptotic and oxidative behavior, complex **4** was chosen as representative. Using DHR-123 as a probe for ROS detection, we found that when NAC (1 mM) or Trolox (100 μ M) were added to cultures before

adding complex **4**, the oxidation state of the probe was reduced to levels comparable to those of nontreated control cells (Figure 5A). However, when we analyzed the survival of cells cotreated with NAC or Trolox and complex **4**, we found that while NAC treatment was able to prevent cell death and PARP cleavage, Trolox was not (Figures 5B and 5C). Indeed, the cells exhibited comparable mortality and PARP cleavage regardless of Trolox presence (Figures 5B–5D). These apparently contradictory data suggest that caspase activation, that ultimately causes PARP cleavage, is not directly triggered by ROS, and indicate that gold(III) compounds might promote cell death by other mechanisms that are counteracted by NAC.

Molecular Targets at Mitochondrial and Cytosolic Levels

Thioredoxin reductase (TrxR) appears to be a very specific intracellular target for antitumor agents. In particular, the mitochondrial isoform may be of potential interest regarding the role of these organelles in the apoptotic process, and previous reports indicate that both gold(I) and gold(III) complexes are highly specific inhibitors of mitochondrial thioredoxin reductase [22]. Thioredoxin reductase is a selenoenzyme with a selenol group in the active site at the C terminus of the enzyme [29]. Gold compounds preferentially interact with this site since selenol displays a greater affinity toward heavy metals [30].

On the basis of these considerations, our gold(III)-dithiocarbamate derivatives were tested to study their potential inhibitory effect on this selenoenzyme. The inhibitory activity of complexes **1–4** on both cytosolic (TrxR1) and mitochondrial (TrxR2) thioredoxin reductase is reported in Figure 6. The cytosolic isoform (Figure 6A) is particularly sensitive to the action of gold(III) compounds, all of them being inhibitory agents at nanomolar level, exhibiting IC₅₀ values ranging from 5.67 nM (complex **1**) to 17.01 nM (complex **3**). Mitochondrial thioredoxin reductase (Figure 6B) seems to be less sensitive to the treatment, with IC₅₀ values ranging from 24.74 nM (complex **1**) to

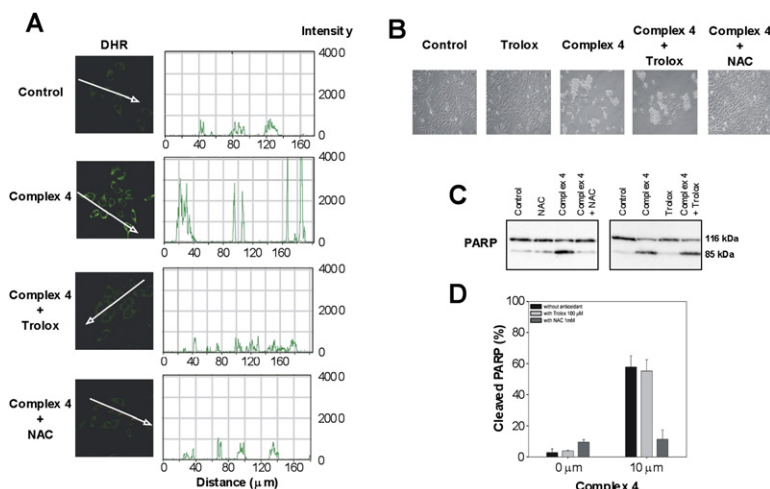


Figure 5. Effect of Treatment with the Antioxidants Trolox and NAC on ROS Generation in Cell Death

(A) HeLa cells were treated and examined for ROS generation as described in Figure 4C. Graphs report the profile of DHR-123 relative intensity quantified using the Zeiss Profile software. Profiles are referred to the signals along a line traced across few cells. When present, Trolox (100 μM) or NAC (1 mM) were added for 1 h and 18 h, respectively, before treatment with both DHR-123 and complex 4 (10 μM).

(B) Phase-contrast microscopy representative pictures showing HeLa cells pretreated for 1 h with Trolox (100 μM) or 18 h with NAC (1 mM) and then incubated for additional 24 h in medium containing 10 μM complex 4. Original magnification = 100×. Quantification of apoptosis through PARP cleavage determination. (C) PARP cleavage was analyzed by western blot as described in the Experimental Procedures.

(D) Graph showing the percentage of PARP cleavage calculated as the ratio between densitometrical values of cleaved and uncleaved bands × 100. Values are given as means ± SE of at least three independent experiments.

35.87 nM (complex 4). However, in both cases the inhibitory effect is massive, and it is likely to be due to the interaction with the selenol residue present in the active site of thioredoxin reductase. In fact, thioredoxin reductase obtained from *E. coli*, lacking the cysteine/selenocysteine motif at the C terminus, is almost totally insensitive to the gold(III) complexes (Figure 6C). Glutathione reductase is also unaffected by the treatment with complexes 1–4, and this is in agreement with the fact that, although glutathione reductase is a protein structurally and functionally close to thioredoxin reductase and belongs to the same family of the pyridine nucleotide oxidoreductase, it lacks selenol at the catalytic site (Figure 6D). In fact, as previously reported, it requires much greater concentrations of auranofin and other gold compounds to be inhibited [31].

Analysis of ERK Phosphorylation

Mammalian thioredoxin reductase is a key enzyme for maintenance of intracellular reduced environment since it acts as a direct antioxidant of thioredoxin (Trx). Impairment of TrxR will lead to increased levels of oxidized Trx. Trx protects cells from a variety of oxidative stresses by regulating the redox state and activity of many cellular proteins that control cell growth. In the reduced form, Trx associates with apoptosis signal-regulating kinase-1/mitogen-activated protein kinase kinase kinase (ASK-1/MAPKKK). Oxidation of Trx results in its dissociation and consequent activation of the MAPK pathway [32].

Recent studies suggest that apoptotic stimuli are transmitted to caspases through the activation of MAPKKK [33], and it is also believed that, depending on the length of MAPKs activation (e.g., transient or prolonged), they might trigger cell proliferation or death [34]. Furthermore, it was shown that ROS, in particular hydrogen peroxide,

might lead to the activation of extracellular signal-regulated kinases (ERKs) [35].

In order to investigate the influence of our gold(III) complexes on MAPK signaling, we examined the activation of ERK1 (p44) and ERK2 (p42). Kinetic studies showed that treatment with complex 4 rapidly increases phospho-ERK levels (Figure 6E). Nevertheless, when cells were treated in the presence of Trolox, no significant increase in ERK phosphorylation was observed (Figure 6F). These results might indicate that hydrogen peroxide accumulation influences MAPK signaling. Since the antioxidants Trolox and NAC showed different effects on cell survival and PARP cleavage in long-term treatment (Figures 5B–5D), we also studied the ERK phosphorylation state in cells treated with complex 4 for 24 hr in the presence or absence of either Trolox or NAC. We found that Trolox was not able to block the increase of phospho-ERK (Figure 6G); on the contrary, NAC treatment completely blocked the induction of phospho-ERK by complex 4 (Figure 6H). These data may explain the different behavior of the two antioxidants on cell survival. It is worth noting that NAC, even at relatively high concentration, does not alter the inhibitory effect of gold(III)-dithiocarbamate complexes on thioredoxin reductase.

DISCUSSION

The here investigated gold(III) complexes 1–4 were recently proved to be 1- to 4-fold more cytotoxic *in vitro* than cisplatin, even toward human tumor cell lines intrinsically resistant to cisplatin itself [15]. Moreover, they appeared to induce cell death also on cisplatin-resistant cell lines, with activity levels comparable to those on the corresponding cisplatin-sensitive cell lines, ruling out the

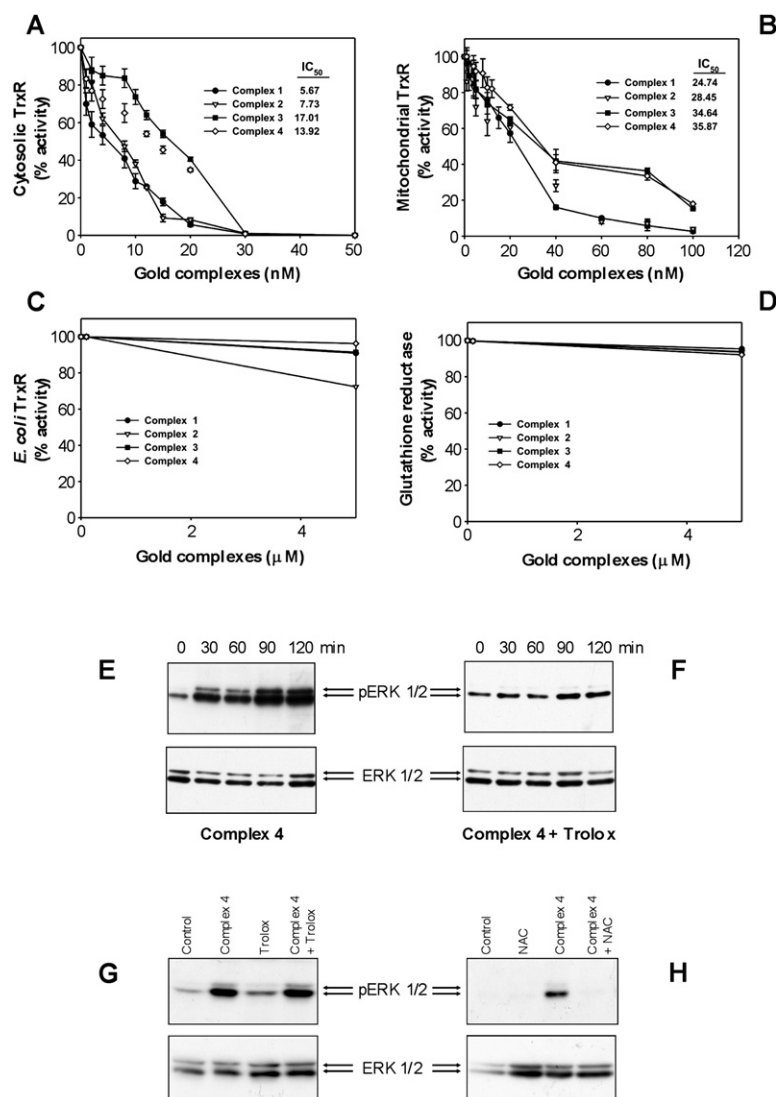


Figure 6. Effect on Thioredoxin and Glutathione Reductase and Induction of ERK Phosphorylation

Cytosolic (A), mitochondrial (B) and *E. coli* (C) thioredoxin reductases and glutathione reductase (D) were incubated as described in the Experimental Procedures. Gold(III) complexes were added at the indicated concentrations. The final concentrations of the enzymes were 2.1 and 3.8 nM for TrxR1 and TrxR2, respectively. *E. coli* thioredoxin reductase was 40.2 μg/ml while glutathione reductase was 4.3 nM. The inhibitory effect of each tested compound was evaluated in comparison with the corresponding control (untreated thioredoxin and glutathione reductase). Dose-response curves were calculated over the indicated range of concentrations, enabling IC₅₀ values to be obtained. Values are given as means ± SE of at least three independent experiments. HeLa cells (1.5×10^5 cells per well) were incubated with complex 4 (10 μM) for 30 min to 3 h in the presence (F) or not (E) of 100 μM Trolox or for 24 h with 100 μM Trolox (G) or 1 mM NAC (H). At the end of treatments, aliquots of protein lysate, corresponding to 4.5×10^4 cells, were subjected to SDS-PAGE in 10% gel. Proteins were then transferred to PVDF and immunodecorated using anti-ERK and anti-phospho-ERK antibodies. Blots are representative of at least two independent experiments.

occurrence of crossresistance phenomena and supporting the hypothesis of a different mechanism of action [15]. The chemical characterization carried out in aqueous solution allowed us to establish that they are reasonably stable within a physiologically relevant environment, an essential prerequisite for any further pharmacological evaluation [16]. Moreover, they show high reactivity toward some biologically relevant isolated macromolecules, and dramatically inhibit both DNA and RNA synthesis, and induce DNA lesions with a faster kinetics than cisplatin. Nevertheless, they also induce a strong and fast hemolytic effect (compared to cisplatin), suggesting that intracellular DNA might not represent their primary or exclusive biological target [16]. These encouraging results prompted us to carry out further investigations aimed at elucidating their mechanism of action.

Although gold drugs have been in clinical use for over 70 years, their exact mechanism of action is on debate, as their specific cellular targets are still unclear. Recent studies showed that mitochondria may play a major role

in their mechanism of cytotoxicity and antitumor activity [6]. Gold(III) complexes were generally proved to be less effective than gold(I) derivatives, such as auranofin, in stimulating mitochondrial swelling, and this might depend on the different permeability characteristics of these complexes [22]. Moreover, the production of hydrogen peroxide by gold(I) compounds was already observed with auranofin both in isolated mitochondria and in cellular systems [36]. We demonstrate that also gold(III) dithiocarbamate derivatives are able to spark the production of this reactive oxygen species. Furthermore, due to the lack of effect of these complexes on respiration it is reasonable to conclude that the observed increase in hydrogen peroxide is essentially due to their inhibitory effect on thioredoxin reductase rather than to stimulation of the mitochondrial electron transport chain.

Besides the strong impairment on thioredoxin reductase, we found that gold(III)-dithiocarbamate complexes increase the levels of phosphorylated ERK1/2 in HeLa cells. Activation of the ERK1/2 pathway by reactive

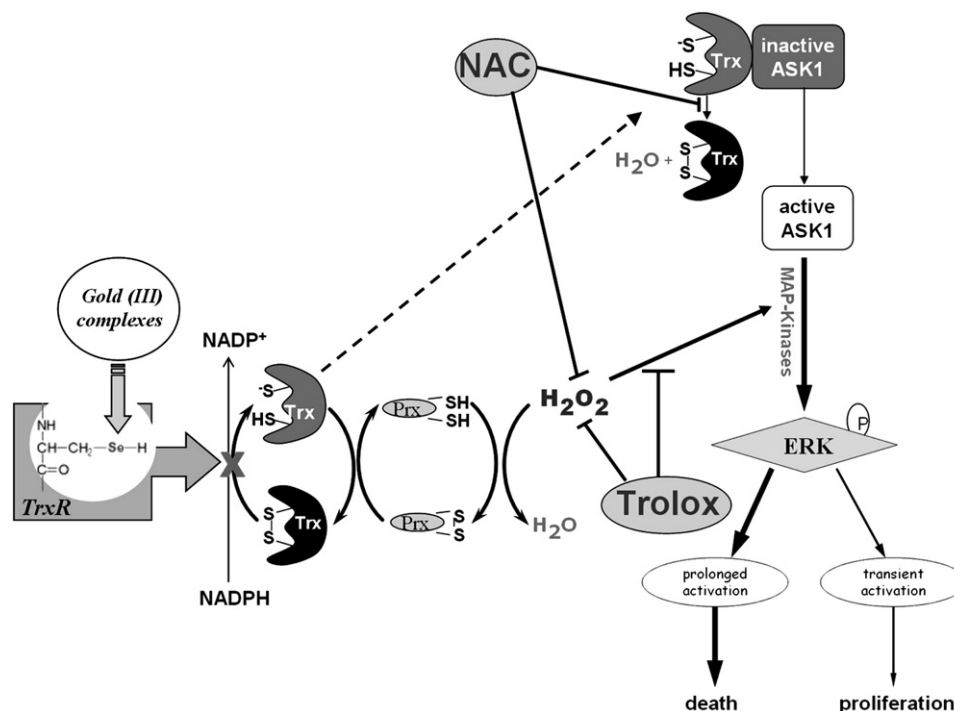


Figure 7. Proposed Model of the Molecular Mechanisms Underlying Gold(III)-Dithiocarbamate Derivatives-Induced Cell Death

oxygen species has been reported by several groups [37–39]. Nevertheless, more recently it has been reported that ERK1/2 play a crucial role in the signaling downstream ASK1. Indeed, apoptosis induced by the iron chelator deferoxamine [40] or acrolein [41] is mediated by both p38 and ERK activation in keratinocytes. Interestingly, acrolein is a potent inhibitor of thioredoxin reductase [42]. Moreover, it was shown that in cultured cerebellar granule neurons in low potassium-induced apoptosis the ERK phosphorylation was activated by the ASK1-p38MAPK pathway [43]. Activation of MAP kinases as a mechanism of apoptosis induced by gold(I) compounds was also suggested by Park and coworkers [33]. However, they reported that in promyelocytic leukemia HL60 cells treated with auranofin the major kinase involved was p38-MAPK, whereas activation of ERK was independent of auranofin concentration. These data, apparently in conflict with our findings, also indicate a direct involvement of ASK1 in gold compounds-induced cell death. The activation of different effector kinases downstream of ASK1 might be explained as the results of the different cell system used and the experimental timing.

The fact that incubation with the scavenger Trolox can reduce phospho-ERK levels after short-term treatment (3 h) with the investigated gold(III) complexes but it is unable to block ERK activation, as well as cell toxicity and PARP cleavage, when the treatment is prolonged for 24 h, suggests that our compounds trigger ERK phosphorylation mainly through ASK1 pathway deregulation. This hypothesis is supported by the results obtained by using NAC as an alternative antioxidant, and the reported capa-

bility of NAC itself to prevent dissociation of the Trx-ASK complex [44], most likely by maintaining thioredoxin reduced. In addition, these data strongly indicate that sustained and long-lasting stimulation of ERK phosphorylation is directly involved in cell death. Indeed, several groups reported that ERK1/2 play important roles not only in cell proliferation and survival, but also in the progression of apoptosis [45, 46]. The mechanisms by which ERK induces apoptosis are not completely clarified yet, but it is believed that might occur at many different levels involving both the extrinsic and intrinsic apoptotic pathways [45]. For instance, inhibition of ERK phosphorylation decreases Bax expression [39] and, in addition, ERK1/2 activity is downregulated by the ubiquitin/proteasome system [47]. These results rationalize recent observations obtained with gold(III)-methylsarcosinedithiocarbamate complexes indicating that they both upregulate Bax and downregulate Bcl2 [18], whereas complex 1 exerts an inhibitory action on the proteasome system [20]. Hence, proteasome inhibition can also explain the observed long-lasting persistence of phosphorylated ERK1/2.

Based on these results, we propose a working model for the mechanism of action of our gold(III)-dithiocarbamate complexes (Figure 7). As already reported for some organogold(III) compounds [24], complexes 1–4 can inhibit thioredoxin reductase by irreversible covalent binding to its catalytic site. This hampers the function of both mitochondrial and cytosolic thioredoxin reductases that act as mediators of electron flow from NADPH to peroxiredoxins through Trx, and lead to an increase in the oxidized form of Trx and to the accumulation of hydrogen peroxide.

Both the events can improve the levels of phospho-ERK. Indeed, it has been reported that hydrogen peroxide accumulation can trigger ERK1/2 phosphorylation [48]. On the other hand, oxidation of Trx will bring on dissociation of the complex Trx-ASK1 and activation of MAPK system observed as subsequent ERK1/2 phosphorylation [49]. Thus, we hypothesize that a persistent ERK1/2 activation triggered at first by accumulation of hydrogen peroxide and then by activation of ASK-1 may be responsible for cell death.

SIGNIFICANCE

Gold compounds possess a variety of therapeutic potentials ranging from attenuation of inflammation, suppression of autoimmunity, and promising antitumor activity. Due to their chemical similarity to platinum(II) compounds, it was believed that gold(III) compounds might have DNA as their biological target. However, gold(III) complexes have been reported to interact also with several other cellular components, and recent data indicated mitochondria as potential targets. Nevertheless, so far the mechanism of action of gold(III) compounds is unclear and there is little understanding of how they can elicit their activity.

By means of cellular, biochemical, and molecular approaches, we analyzed the mechanism of action of recently synthesized gold(III)-dithiocarbamate derivatives. These compounds are able to trigger cell death, to induce ROS generation, to modify some mitochondrial functions, and to inactivate both cytosolic and mitochondrial thioredoxin reductases. Besides the impairment of TrxR, they induce elevated and long-lasting levels of phosphorylated ERK1/2; persistent high levels of phosphorylated ERK might be the cause of cell death. Thus, it is worthwhile to envisage that gold(III) complexes favor the dissociation of the Trx-ASK complex and the consequent prolonged activation of MAPK kinase pathways by inhibiting the TrxR/Trx redox system. This hypothesis is further supported by the finding that both ERK phosphorylation and cell death were inhibited by treatment with the antioxidant NAC, whereas the peroxyl scavenger Trolox was ineffective. Indeed, it has been reported that NAC itself prevents the dissociation of the complex Trx/ASK kinase, most likely by keeping Trx in the reduced state.

Drugs that target specifically TrxR are of undoubted therapeutic relevance given that many tumors exhibit increased levels of TrxR or Trx, which might contribute to resistance of cancer to therapy by scavenging ROS eventually generated by various anticancer agents.

EXPERIMENTAL PROCEDURES

Materials

Human cervical carcinoma HeLa cell line was obtained from the American Type Culture Collection. Cisplatin (Bristol-Myers Squibb), Dulbecco's modified Eagle medium (DMEM, Sigma Aldrich), fetal bovine serum (FBS, Gibco), L-glutamine (Gibco), penicillin (Pharmacia), streptomycin (Bristol-Myers Squibb), phosphate buffered saline solution (PBS, Sigma), low fat milk (Roche), rotenone, oligomycin, antimycin,

carbonylcyanide *m*-chlorophenylhydrazone (CCCP), horseradish peroxidase (HRP), *N*-acetyl-L-cysteine (NAC), 5,5'-dithiobis-(2-nitrobenzoic acid) (DTNB) and Rhodamine-123 were purchased from Sigma. 6-Hydroxy-2,5,7,8-tetramethylchroman-2-carboxylic acid (Trolox) was purchased from Fluka. Dihydrorhodamine-123 (DHR-123) and 10-acetyl-3,7-dihydroxyphenoxazine (Amplex Red) were purchased from Invitrogen-Molecular Probes. All reagents and solvents were of high purity and were used as purchased without any further purification.

Gold(III) complexes **1–4** were synthesized as previously described [15]. Before use, gold(III) complexes were dissolved in DMSO just before the experiments; calculated amounts of drug solutions were then added to the proper medium, to a final organic solvent concentration lower than 0.5% (v/v). All the tested complexes were proved, by ¹H NMR studies, to be stable in DMSO over 48 h [15].

X-Ray Crystallography

Crystals of complex **4** suitable for X-ray crystal-structure determination were obtained from an acetone/hexane (1:1) solution at 4°C. Diffraction data were collected using a Bruker Smart Apex CCD diffractometer equipped with an Oxford Cryosystems low-temperature device operating at 150 K. The diffraction pattern was indexed with two orientation matrices related via a 2-fold rotation about the [100] direction (CELL_NOW [50]). Reflections from both domains were integrated simultaneously and used in refinement (SAINT [51]). An absorption correction was performed with the multiscan procedure TWINABS [52]. The structure was solved by Patterson methods (DIRDIF) [53], and refined against F² using SHELXL-97 [54]. H atoms were placed in calculated positions. The terminal EtO- group is disordered over two orientations to avoid a close contact across an inversion center. The occupancies were fixed at 0.5, and similarity restraints were applied to the bond distances and angles in the part-weight fragments. The twin scale factor refined to 0.523(15). X-ray crystallographic data are available in the Supplemental Data. The crystal structure of complex **4** has been deposited at the Cambridge Crystallographic Data Centre and allocated the deposition number CCDC641437. These data can be obtained free of charge from The Cambridge Crystallographic Data Centre via http://www.ccdc.cam.ac.uk/data_request/cif.

Determination of Apoptotic Activity in HeLa Cells

HeLa cells were cultured at 37°C in 5% CO₂ atmosphere in Dulbecco's modified Eagle medium supplemented with 10% fetal bovine serum, 2 mM L-glutamine and antibiotics (200 units/ml penicillin, 150 units/ml streptomycin). For apoptosis analysis, cells were seeded into 6-well plates at a density of 1.5 × 10⁵ cells per well, and exposed to the gold(III) complexes or cisplatin. After 24 h of incubation, cell death was evaluated by visual inspection using an Olympus phase-contrast microscope. After microscope observation, cells were collected and subjected to SDS-polyacrylamide gel electrophoresis (SDS-PAGE) and western blot analysis (see below).

SDS-PAGE and Western Blot Analysis

After treatment, all cells, including floating dead ones, were collected, and total proteins were extracted in Laemmli buffer (LB-1X: 50 mM Tris-HCl [pH 6.8], 2% SDS, 10% glycerol, 1% β-mercaptoethanol, 0.05% bromophenol blue) supplemented with a cocktail of protease inhibitors (Roche) and 50 mM sodium fluoride. Aliquots of lysate were subjected to SDS-PAGE. Proteins were then transferred to polyvinylidene fluoride (PVDF) membranes (Amersham) and probed with the specific antibodies. The following antibodies were utilized: rabbit polyclonal anti-PARP, mouse monoclonal anti-phospho-ERK1/2, and rabbit polyclonal anti-total ERK1/2 (Cell Signaling Technology) at the manufacturer's indicated concentrations. Secondary HRP-conjugated antibodies (sheep anti-mouse or donkey anti-rabbit, Amersham) were used at a concentration of 1:10,000 in PBS-milk (5% powdered skimmed milk in PBS with 0.05% Tween). Membranes were developed using the enhanced chemiluminescence detection system ECL-Plus (Amersham). Densitometric analysis was carried out using the Multianalyst Biorad analysis software.

Preparation of Rat Liver Mitochondria and Submitochondrial Particles

Mitochondria were prepared from rat liver by differential centrifugation essentially according to Myers et al. [55] in a medium containing 220 mM mannitol, 70 mM sucrose, 1 mM EDTA and 5 mM HEPES (pH 7.0). EDTA was omitted in the final washing and in the mitochondrial suspension. Mitochondrial proteins were estimated with the biuret procedure using BSA as standard [56].

To obtain submitochondrial particles, mitochondria were diluted to about 20 mg/ml with 25 mM Tris-HCl buffer (pH 8.0) and sonicated twice for 30 s. The suspension was then centrifuged at 10,000 × g for 10 min to remove the unbroken mitochondria, the pellet was discarded, and the supernatant again centrifuged at 105,000 × g for 30 min. The obtained pellet, after washing, was suspended in a small volume of the same medium used for mitochondria.

Measurement of Oxygen Uptake

Rat liver mitochondria (1 mg/ml) or submitochondrial particles (0.5 mg/ml) were treated with complexes 1–4 at 25°C in 0.1 M sucrose, 50 mM KCl, 1 mM MgCl₂, 1 mM NaH₂PO₄, 20 mM HEPES/Tris-HCl buffer (pH 7.4), 1 mM EGTA, and 5 mM glutamate plus 5 mM malate as substrates. State 3 respiration was initiated by adding 0.3 mM ADP. For submitochondrial particles either 7.5 mM succinate or 0.75 mM NADH were used as substrate. Oxygen uptake was estimated polarographically at 25°C using a Clark-type oxygen electrode (Yellow Springs) [57] fitted in a water-jacketed chamber with continuous stirring. Mitochondria with respiratory control ratio of 4 or greater were utilized. To validate the oxygen uptake experiments, positive controls were run in the presence of 0.5 μM CCCP to obtain the maximal respiration and 1 μM antimycin A to completely inhibit oxygen consumption (not shown).

Measurement of Membrane Potential

Mitochondrial membrane potential was estimated by means of the fluorescent dye rhodamine-123 according to Emaus et al. [58]. Mitochondrial proteins (0.3 mg/ml) were incubated at 25°C in 100 mM sucrose, 50 mM KCl, 20 mM HEPES/Tris-HCl buffer (pH 7.4), 1 mM NaH₂PO₄, 1 mM MgCl₂, 6 μM rotenone, and 0.3 μM rhodamine-123. Complexes 1–4 were then added at increasing concentrations. Fluorescence was estimated in a microplate reader (Ascent FL, Labsystem) at 485 nm (excitation wavelength) and 527 nm (emission wavelength) in a final volume of 250 μl. To validate the estimation, a positive control with the uncoupler CCCP (0.5 μM) showing a rapid and complete collapse of membrane potential was performed (not shown).

Estimation of Mitochondrial Swelling

Rat liver mitochondria (0.5 mg/ml) were incubated at 25°C in 0.22 M mannitol, 71 mM sucrose, 5 mM HEPES/Tris buffer (pH 7.4), 5 mM succinate, 5 μM rotenone, and 3 μM oligomycin. Swelling was triggered by the addition of complexes 1–4. Mitochondrial swelling was estimated as absorbance decrease at 540 nm using a Lambda-2 UV/VIS spectrophotometer (Perkin-Elmer). To validate the experimental procedure, mitochondrial swelling was triggered with 50 μM CaCl₂ and 1 mM Na,K-phosphate as positive control (not shown).

Determination of ROS Formation by Isolated Rat Liver Mitochondria

Rat liver mitochondria (1 mg/ml) were incubated at 30°C in 0.1 M sucrose, 50 mM KCl, 0.5 mM Na,K-phosphate, 20 mM HEPES/Tris-HCl buffer (pH 7.4). Hydrogen peroxide formed by exposure of isolated mitochondria to complexes 1–4 was determined using the fluorogenic probe Amplex Red (10 μM) in the presence of HRP (0.1 unit/ml) according to Mohanty et al. [59]. Fluorescence was followed in a Cary Eclipse Varian spectrofluorometer at 544 nm (excitation wavelength) and 620 nm (emission wavelength).

Determination of ROS Accumulation in HeLa Cells

Cells were seeded into Lab-Tek Chambered Glasses, 11 × 22 mm 4-well plates at a density of 5 × 10⁴ cells per well. After 24 h of incubation, cells were loaded with the oxidation-sensitive probe DHR-123 (5 μM) for 30 min, and then exposed to complexes 1–4 for an additional 30 min, in the presence or absence of the antioxidants Trolox or NAC. At the end of treatment, cells were examined for ROS generation using a Zeiss LSM-510 confocal laser microscope equipped with a CO₂- and temperature-controlled chamber.

Purification of Thioredoxin Reductase and Estimation of Thioredoxin Reductase and Glutathione Reductase Activities

Cytosolic thioredoxin reductase (TrxR1) was prepared from rat liver according to Luthman et al. [60]. Mitochondrial thioredoxin reductase (TrxR2) was prepared from rat liver mitochondria according to Rigobello et al. [61]. *E. coli* thioredoxin reductase was prepared according to Williams et al. [62], whereas yeast glutathione reductase was used as purchased (Sigma). The protein content of isolated enzymes was estimated according to Lowry et al. [63]. Thioredoxin reductase activity was measured at 25°C in 0.2 M Na,K-Pi buffer (pH 7.5), 2 mM EDTA, and 0.25 mM NADPH and started by the addition of 2 mM DTNB and followed spectrophotometrically at 412 nm. Glutathione reductase activity was assayed at 25°C in 0.1 M Tris-HCl (pH 8.1) and 0.2 mM NADPH. Reactions were initiated by 1 mM GSSG and followed spectrophotometrically at 340 nm. In both thioredoxin and glutathione reductase assays the various gold(III) complexes were added after 5 min of incubation and, after 5 additional minutes, the reactions were initiated by DTNB and GSSG, respectively.

Statistical Analyses

All the values are given as means ± SE of not less than three measurements (unless otherwise stated). Multiple comparisons were made by one-way analysis of variance followed by the Tukey-Kramer multiple comparison test.

Supplemental Data

The Supplemental Data include details of the intermolecular interactions and disorder in the X-ray structure of complex 4 and X-ray crystallographic data in CIF format and can be found at <http://www.chembiol.com/cgi/content/full/14/10/1128/DC1/>.

ACKNOWLEDGMENTS

This work was partially supported by Ministero dell'Università e della Ricerca Scientifica e Tecnologica (Pharmacological and diagnostic properties of metal complexes). We thank Fondazione Italiana per la Ricerca sul Cancro—FIRC (Fellowship for L.P.), and European Union (Marie Curie Fellowship for L.R.) for financial support.

Received: May 10, 2007

Revised: July 26, 2007

Accepted: August 10, 2007

Published: October 26, 2007

REFERENCES

- Best, S.L., and Sadler, P.J. (1996). Gold drugs: mechanism of action and toxicity. *Gold Bull.* 29, 87–93.
- Shaw, C.F., III. (1999). Gold-based therapeutic agents. *Chem. Rev.* 99, 2589–2600.
- Ahmad, S. (2004). The chemistry of cyano complexes of gold(I) with emphasis on the ligand scrambling reactions. *Coord. Chem. Rev.* 248, 231–243.
- Ahmad, S., Isab, A.A., Ali, S., and Al-Arfaj, A.R. (2006). Perspectives in bioinorganic chemistry of some metal based therapeutic agents. *Polyhedron* 25, 1633–1645.

5. Shaw, C.F., III. (1999). The biochemistry of gold. In *Gold-Progress in Chemistry, Biochemistry and Technology*, H. Schmidbaur, ed. (Chichester, United Kingdom: John Wiley & Sons), pp. 259–308.
6. McKeage, M.J., Maharaj, L., and Berners-Price, S.J. (2002). Mechanisms of cytotoxicity and antitumor activity of gold(I) phosphine complexes: the possible role of mitochondria. *Coord. Chem. Rev.* 232, 127–135.
7. Tiekink, E.R.T. (2002). Gold derivatives for the treatment of cancer. *Crit. Rev. Oncol. Hematol.* 42, 225–248.
8. Messori, L., and Marcon, G. (2004). Gold complexes as antitumor agents. In *Metal Ions in Biological Systems - Metal Complexes in Tumor Diagnosis and as Anticancer Agents*, A. Sigel and H. Sigel, eds. (Basel, Switzerland: FontisMedia S.A. and Marcel Dekker Inc.), pp. 385–424.
9. Kostova, I. (2006). Gold coordination complexes as anticancer agents. *Anticancer Agents Med. Chem.* 6, 19–32.
10. Ward, J.R. (1988). Role of disease-modifying antirheumatic drugs versus cytotoxic agents in the therapy of rheumatoid arthritis. *Am. J. Med.* 85, 39–44.
11. Messori, L., Abbate, F., Marcon, G., Orioli, P., Fontani, M., Mini, E., Mazzei, T., Carotti, S., O'Connell, T., and Zanello, P. (2000). Gold(III) complexes as potential antitumor agents: solution chemistry and cytotoxic properties of some selected gold(III) compounds. *J. Med. Chem.* 43, 3541–3548.
12. Marcon, G., Carotti, S., Coronello, M., Messori, L., Mini, E., Orioli, P., Mazzei, T., Cinellu, M.A., and Minghetti, G. (2002). Gold(III) complexes with bipyridyl ligands: solution chemistry, cytotoxicity, and DNA binding properties. *J. Med. Chem.* 45, 1672–1677.
13. Fan, D., Yang, C.T., Ranford, J.D., Vittal, J.J., and Lee, P.F. (2003). Synthesis, characterization, and biological activities of 2-phenylpyridine gold(III) complexes with thiolate ligands. *Dalton Trans.* 17, 3376–3381.
14. Giovagnini, L., Ronconi, L., Aldinucci, D., Lorenzon, D., Sitran, S., and Fregona, D. (2005). Synthesis, characterization, and comparative in vitro cytotoxicity studies of platinum(II), palladium(II), and gold(III) methylsarcosinedithiocarbamate complexes. *J. Med. Chem.* 48, 1588–1595.
15. Ronconi, L., Giovagnini, L., Marzano, C., Bettio, F., Graziani, R., Pilloni, G., and Fregona, D. (2005). Gold dithiocarbamate derivatives as potential antineoplastic agents: design, spectroscopic properties, and in vitro antitumor activity. *Inorg. Chem.* 44, 1867–1881.
16. Ronconi, L., Marzano, C., Zanello, P., Corsini, M., Miolo, G., Maccà, C., Trevisan, A., and Fregona, D. (2006). Gold(III) dithiocarbamate derivatives for the treatment of cancer: solution chemistry, DNA binding, and hemolytic properties. *J. Med. Chem.* 49, 1648–1657.
17. Blank, C.F., and Dabrowiak, J.C. (1984). Absorption and circular dichroism studies of a gold(I)-DNA complex. *J. Inorg. Biochem.* 21, 21–29.
18. Aldinucci, D., Lorenzon, D., Stefani, L., Giovagnini, L., Colombatti, A., and Fregona, D. (2007). Antiproliferative and apoptotic effects of two new gold(III) methylsarcosinedithiocarbamate derivatives on human acute myeloid leukemia cells in vitro. *Anticancer Drugs* 8, 323–332.
19. Eastman, A. (1999). The mechanism of action of cisplatin: from adducts to apoptosis. In *Cisplatin. Chemistry and Biochemistry of a Leading Anticancer Drug*, B. Lippert, ed. (Zurich, Switzerland: VCHA & Wiley-VCH), pp. 111–134.
20. Milacic, V., Chen, D., Ronconi, L., Landis-Piwowar, K.R., Fregona, D., and Dou, Q.P. (2006). A novel anticancer gold(III) dithiocarbamate compound inhibits the activity of a purified 20S proteasome and 26S proteasome in human breast cancer cell cultures and xenografts. *Cancer Res.* 66, 10478–10486.
21. Rigobello, M.P., Scutari, G., Boscolo, R., and Bindoli, A. (2002). Induction of permeability transition by auranofin, a gold(I)-phosphine derivative. *Brit. J. Pharm.* 136, 1162–1168.
22. Rigobello, M.P., Messori, L., Marcon, G., Cinellu, M.A., Bragadin, M., Folda, A., Scutari, G., and Bindoli, A. (2004). Gold complexes inhibit mitochondrial thioredoxin reductase. Consequences on mitochondrial functions. *J. Inorg. Biochem.* 98, 1634–1641.
23. Coronello, M., Mini, E., Caciagli, B., Cinellu, M.A., Bindoli, A., Gabbiani, C., and Messori, L. (2005). Mechanisms of cytotoxicity of selected organogold(III) compounds. *J. Med. Chem.* 48, 6761–6765.
24. Engman, L., McNaughton, M., Gajewska, M., Kumar, S., Birmingham, A., and Powis, G. (2006). Thioredoxin reductase and cancer cell growth inhibition by organogold(III) compounds. *Anticancer Drugs* 17, 539–544.
25. Ronconi, L., Maccato, C., Barreca, D., Saini, R., Zancato, M., and Fregona, D. (2005). Gold(III) dithiocarbamate derivatives of N-methylglycine: an experimental and theoretical investigation. *Polyhedron* 24, 521–531.
26. Rosenthal, D.S., Simbulan-Rosenthal, C.M., Smith, W.J., Benton, B.J., Ray, R., and Smulson, M.E. (2000). Poly (ADP-ribose) polymerase is an active participant in programmed cell death and maintenance of genomic stability. In *Cell Death: The Role of PARP*, C. Szabo, ed. (Boca Raton, FL: CRC Press), pp. 227–249.
27. Kaufmann, S.H., Desnoyers, S., Ottaviano, Y., Davidson, N.E., and Poirier, G.G. (1993). Specific proteolytic cleavage of poly(ADP-ribose) polymerase: an early marker of chemotherapy-induced apoptosis. *Cancer Res.* 53, 3976–3985.
28. Green, D.R., and Reed, J.C. (1998). Mitochondria and apoptosis. *Science* 281, 1309–1312.
29. Sandalova, T., Zhong, L., Lindqvist, Y., Holmgren, A., and Schneider, G. (2001). Three-dimensional structure of a mammalian thioredoxin reductase: Implications for mechanism and evolution of a selenocysteine-dependent enzyme. *Proc. Natl. Acad. Sci. USA* 98, 9533–9538.
30. Klayman, D.L. (1973). Selenols and their derivatives (excluding selenides). In *Organic Selenium Compounds: Their Chemistry and Biology*, D.L. Klayman and W.H.H. Gunther, eds. (New York, USA: John Wiley & Sons), pp. 67–122.
31. Gromer, S., Arscott, L.D., Williams, C.H., Jr., Schirmer, R.H., and Becker, K. (1998). Human placenta thioredoxin reductase. Isolation of the selenoenzyme, steady state kinetics, and inhibition by therapeutic gold compounds. *J. Biol. Chem.* 273, 20096–20101.
32. Zhang, R., Al-Lamki, R., Bai, L., Streb, J.W., Miano, J.M., Bradley, J., and Min, W. (2004). Thioredoxin-2 inhibits mitochondria-located ASK1-mediated apoptosis in a JNK-independent manner. *Circ. Res.* 94, 1483–1491.
33. Park, S.J., and Kim, I.S. (2005). The role of p38 MAPK activation in auranofin-induced apoptosis of human promyelocytic leukaemia HL-60 cells. *Br. J. Pharmacol.* 146, 506–513.
34. Sakon, S., Xue, X., Takekawa, M., Sasazuki, T., Okazaki, T., Kojima, Y., Piao, J.H., Yagita, H., Okumura, K., Doi, T., and Nakano, H. (2003). NF-kappaB inhibits TNF-induced accumulation of ROS that mediate prolonged MAPK activation and necrotic cell death. *EMBO J.* 22, 3898–3909.
35. Kim, M.R., Chang, H.S., Kim, B.H., Kim, S., Baek, S.H., Kim, J.H., Lee, S.R., and Kim, J.R. (2003). Involvements of mitochondrial thioredoxin reductase (TrxR2) in cell proliferation. *Biochem. Biophys. Res. Commun.* 304, 119–124.
36. Rigobello, M.P., Folda, A., Baldoin, M.C., Scutari, G., and Bindoli, A. (2005). Effect of auranofin on the mitochondrial generation of hydrogen peroxide. Role of thioredoxin reductase. *Free Radic. Res.* 39, 687–695.

37. Bhat, N.R., and Zhang, P. (1999). Hydrogen peroxide activation of multiple mitogen-activated protein kinases in an oligodendrocyte cell line: Role of extracellular signal-regulated kinases in hydrogen peroxide-induced cell death. *J. Neurochem.* 72, 112–119.
38. Martindale, J.L., and Holbrook, N.J. (2002). Cellular response to oxidative stress: signaling for suicide and survival. *J. Cell. Physiol.* 192, 1–15.
39. Park, B.G., Yoo, C.I., Kim, H.T., Kwon, C.H., and Kim, Y.K. (2005). Role of mitogen-activated protein kinases in hydrogen peroxide-induced cell death in osteoblastic cells. *Toxicology* 215, 115–125.
40. Lee, S.-K., Jang, H.-J., Lee, H.-J., Lee, J., Jeon, B.-H., Jun, C.-D., Lee, S.-K., and Kim, E.-C. (2006). p38 and ERK MAP kinase mediates iron chelator-induced apoptosis and -suppressed differentiation of immortalized and malignant human oral keratinocytes. *Life Sci.* 79, 1419–1427.
41. Tanel, A., and Averill-Bates, D.A. (2007). P38 and ERK mitogen-activated protein kinases mediate acrolein-induced apoptosis in Chinese hamster ovary cells. *Cell. Signal.* 19, 968–977.
42. Yang, X., Wu, X., Choi, Y.E., Kern, J.C., and Kehrer, J.P. (2004). Effect of acrolein and glutathione depleting agents on thioredoxin. *Toxicology* 204, 209–218.
43. Yamagishi, S., Matsumoto, T., Numakawa, T., Yokomaku, D., Adachi, N., Hatanaka, H., Yamada, M., Shimoke, K., and Ikeuchi, T. (2005). ERK1/2 are involved in low potassium-induced apoptotic signaling downstream of ASK-p38 MAPK pathway in cultured cerebellar granule neurons. *Brain Res.* 1038, 223–230.
44. Hsieh, C.C., and Papacostantinou, J. (2006). Thioredoxin-ASK1 complex levels regulate ROS-mediated p38 MAPK pathway activity in levels of aged and long-lived Snell dwarf mice. *FASEB J.* 20, 259–268.
45. Zhuang, S., and Schnellmann, R.G. (2006). A death-promoting role for extracellular signal-regulated kinase. *J. Pharmacol. Exp. Ther.* 319, 991–997.
46. Cagnol, S., van Obberghen-Schilling, E., and Chambard, J.C. (2006). Prolonged activation of ERK1,2 induces FADD-independent caspase 8 activation and cell death. *Apoptosis* 11, 337–346.
47. Lu, Z., Xu, S., Joazeiro, C., Cobb, M.H., and Hunter, T. (2002). The PHD domain of MEKK1 acts as an E3 ubiquitin ligase and mediates ubiquitination and degradation of ERK1/2. *Mol. Cell* 9, 945–956.
48. McCubrey, J.A., Lahair, M.M., and Franklin, R.A. (2006). Reactive oxygen species-induced activation of the MAP kinase signaling pathways. *Antioxid. Redox Signal.* 8, 1775–1789.
49. Song, J.J., and Lee, Y.J. (2003). Differential role of glutaredoxin and thioredoxin in metabolic oxidative stress-induced activation of apoptosis signal-regulating kinase 1. *Biochem. J.* 373, 845–853.
50. Sheldrick, G.M. (2005). CELL NOW. Program for Unit Cell Determination (Göttingen, Germany: University of Göttingen).
51. Bruker-Nonius (2006). SAINT. Program for cell refinement (Madison, Wisconsin: Bruker-AXS).
52. Sheldrick, G.M. (2005). TWINABS. Program for Performing Absorption Corrections to X-ray Diffraction Patterns Collected from Non-Merohedrally Twinned and Multiple Crystals (Göttingen, Germany: University of Göttingen).
53. Beurskens, P.T., Beurskens, G., Bosman, W.P., de Gelder, R., Garcia-Granda, S., Gould, R.O., Israel, R., and Smits, J.M.M. (1997). The DIRDIF97 Program System. Technical Report of the Crystallography Laboratory (Nijmegen, The Netherlands: University of Nijmegen).
54. Sheldrick, G.M. (1997). SHELXL-97. Program for the refinement of crystal structures (Göttingen, Germany: University of Göttingen).
55. Myers, D.K., and Slater, E.C. (1957). The enzymatic hydrolysis of adenosine triphosphate by rat liver mitochondria. I. Activities at different pH values. *Biochem. J.* 67, 558–572.
56. Gornall, A.G., Bardawill, C.J., and David, M.M. (1949). Determination of serum protein by means of the biuret reaction. *J. Biol. Chem.* 177, 751–766.
57. Estabrook, R.W. (1967). Mitochondrial respiratory control and the polarographic measurement of ADP:O ratios. *Methods Enzymol.* 10, 41–47.
58. Emaus, R.K., Grunwald, R., and Lemasters, J.L. (1986). Rhodamine 123 as a probe of transmembrane potential in isolated rat liver mitochondria: spectral and metabolic properties. *Biochim. Biophys. Acta* 850, 436–448.
59. Mohanty, J.G., Jaffe, J.S., Schulman, E.S., and Raible, D.G. (1997). A highly sensitive fluorescent micro-assay of H₂O₂ release from activated human leukocytes using a dihydroxyphenoxazine derivative. *J. Immunol. Methods* 202, 133–141.
60. Luthman, M., and Holmgren, A. (1982). Rat liver thioredoxin and thioredoxin reductase: purification and characterization. *Biochemistry* 21, 6628–6633.
61. Rigobello, M.P., Callegaro, M.T., Barzon, E., Benetti, M., and Bindoli, A. (1998). Purification of mitochondrial thioredoxin reductase and its involvement in the redox regulation of membrane permeability. *Free Radic. Biol. Med.* 24, 370–376.
62. Williams, C.H., Jr., Zanetti, G., Arscott, L.D., and McAllister, J.K. (1967). Lipoamide dehydrogenase, glutathione reductase, thioredoxin reductase, and thioredoxin. A simultaneous purification and characterization of the four proteins from *Escherichia coli* B. *J. Biol. Chem.* 242, 5226–5231.
63. Lowry, O.H., Rosebrough, N.J., Farr, A.L., and Randall, R.J. (1951). Protein measurement with the Folin phenol reagent. *J. Biol. Chem.* 193, 265–275.

Accession Numbers

The coordinates of complex **4** have been deposited in the Cambridge Crystallographic Data Centre with accession code [CCDC641437](#).